

# Catechol oxidase – structure and activity

## Christoph Eicken\*, Bernt Krebs† and James C Sacchettini\*†

Recently determined structures of copper-containing plant catechol oxidase in three different catalytic states have provided new insights into the mechanism of this enzyme and its relationship to other copper type-3 proteins. Moreover, the active site of catechol oxidase has been found to be structurally conserved with the oxygen-binding site of a molluscan hemocyanin.

### Addresses

\*Department of Biochemistry and Biophysics, Texas A&M University, College Station, Texas 77843-2128, USA

†e-mail: sacchett@tamu.edu

‡Westf. Wilhelms-Universität Münster, Anorganisch-Chemisches Institut, Wilhelm-Klemm-Straße 8, 48149 Münster, Germany; e-mail: krebs@uni-muenster.de

**Current Opinion in Structural Biology** 1999, **9**:677–683

0959-440X/99/\$ – see front matter © 1999 Elsevier Science Ltd. All rights reserved.

### Abbreviations

<b>CO</b>	catechol oxidase
<b>EC</b>	Enzyme Commission
<b>EPR</b>	electron paramagnetic resonance
<b>EXAFS</b>	extended X-ray absorption fine structure
<b>Hc</b>	hemocyanin
<b>ibCO</b>	CO from <i>Ipomoea batatas</i>
<b>lpHc</b>	Hc from <i>Limulus polyphemus</i>
<b>odgHc</b>	Hc from <i>Octopus dofleini</i>
<b>piHc</b>	Hc from <i>Panulirus interruptus</i>
<b>PTU</b>	phenylthiourea
<b>rmsd</b>	root mean square deviation

### Introduction

The class of dicopper proteins containing a single type-3 center has three known members, two of which have been studied extensively: hemocyanin (Hc) and tyrosinase. Both proteins are defined by an antiferromagnetically coupled ( $-2J > 600 \text{ cm}^{-1}$ ), EPR-silent Cu(II) pair and two intensive absorption maxima at  $\lambda \approx 345 \text{ nm}$  ( $\epsilon \approx 19,000 \text{ cm}^{-1}\text{M}^{-1}$ ) and  $\lambda \approx 600 \text{ nm}$  ( $\epsilon \approx 1000 \text{ cm}^{-1}\text{M}^{-1}$ ) upon binding oxygen ([1–3] and references therein). Three different states of the active site have been reported: the oxidized Cu(II) containing *met* form, the oxygenated *oxy* form [ $\text{Cu}^{\text{II}}\text{-O}_2\text{-Cu}^{\text{II}}$ ] and the reduced Cu(I) containing *deoxy* form.

In contrast to Hc, which is a large respiratory protein from arthropods (~75 kDa) and molluscs (~350 kDa polypeptide chain, forming seven functional units) responsible for oxygen transport and/or storage, tyrosinase from fungi and vertebrates has two catalytic activities: the hydroxylation of monophenols (like tyrosine) to *o*-diphenols (cresolase activity) and the oxidation of *o*-diphenols (catechols) to *o*-quinones (catecholase activity). Spectroscopic studies and sequence alignments have suggested that the tyrosinase catalytic dicopper site is similar to that of Hc, which has been structurally characterized by X-ray crystallography [1–4]. Extended X-ray absorption fine structure (EXAFS)

data show similar Cu–Cu distances for both proteins and reveal that the coppers have three histidine ligands [1].

The activity of catechol oxidase (CO), the third member of the type-3 class of dicopper proteins, has been less well studied. Initial EXAFS data on CO from *Lycopus europaeus* revealed a shorter Cu(II)–Cu(II) distance compared with Hc and tyrosinase [5]. In contrast to tyrosinase, CO specificity is limited to *o*-diphenols, which are converted to the quinones. In plants, the highly reactive quinones autopolymerize to form brown polyphenolic catechol melanins [6], a process proposed to protect the damaged plant from pathogens or insects [7,8\*\*]. In addition to its function *in vivo*, the CO reaction is of interest as a medical diagnostic to measure hormonal catecholamines (adrenalin, noradrenaline and dopamine).

The classification and specificity of CO and tyrosinase remains an area of confusion. Originally, they were classified as oxygen oxidoreductases (EC 1.12.18.1). Cresolase activity was later given the classification of monophenol monooxygenase (EC 1.14.18.1) and catecholase activity became diphenol oxygen: oxidoreductase (EC 1.10.3.2) [8\*\*]. Apart from early work on CO from *Populus nigra* [9] and the initial characterization of the *Lycopus* enzyme [10], knowledge about CO has been limited, although the primary structures of numerous polyphenol oxidases have been determined [11,12]. Within the past year, more detailed insights into the mechanisms of COs from *Lycopus europaeus* and *Ipomoea batatas* (sweet potatoes) were gained: substrate specificity, the resulting bioproducts of enzymatic caffeic acid oxidation [13] and spectroscopic studies (UV/Vis, EXAFS, EPR and resonance Raman) [14\*,15] have now been reported.

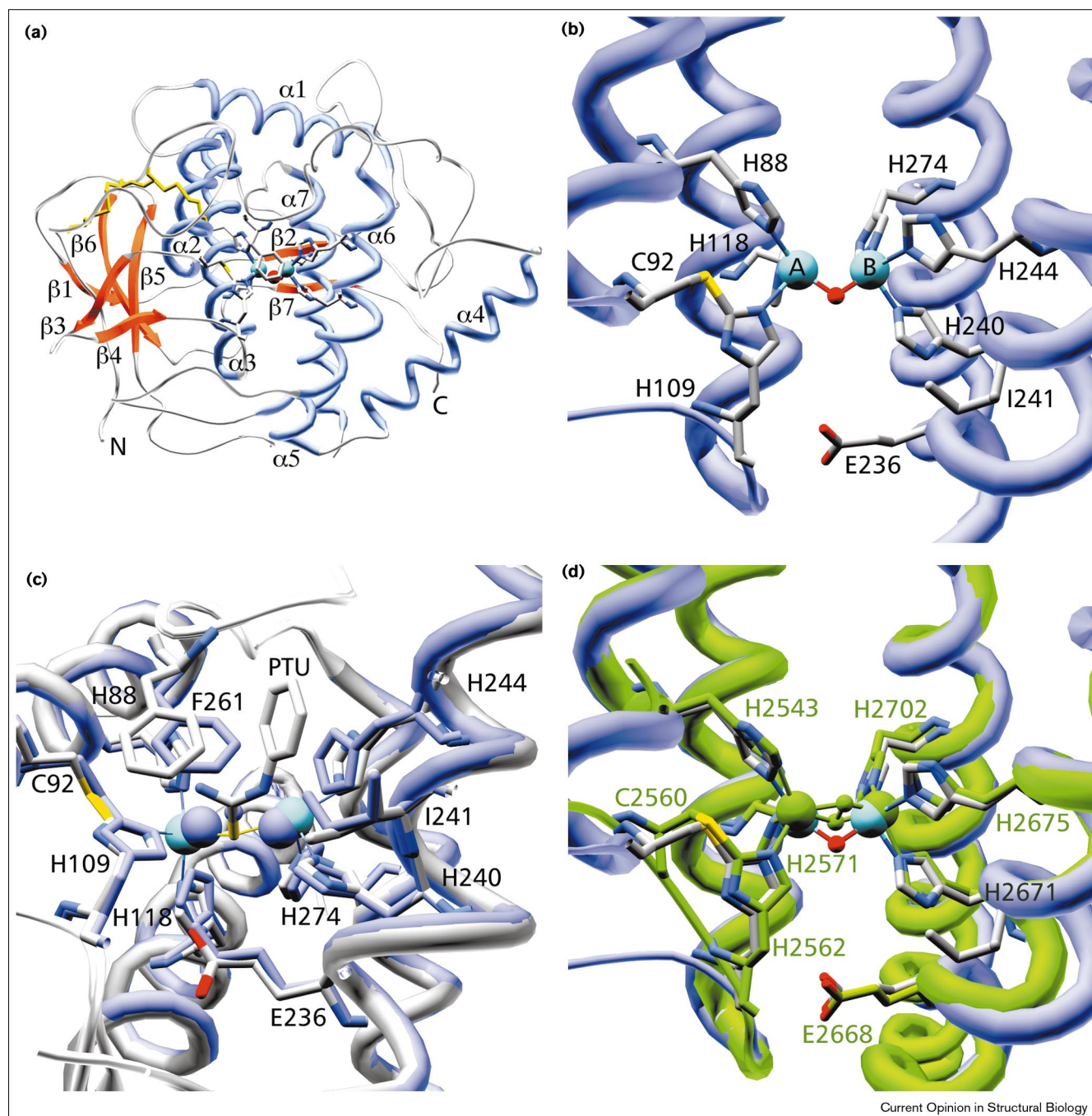
This review focuses on the structure and mechanism of CO from *I. batatas* (ibCO) [16\*\*].

### Crystal structure

The structure of the monomeric 39 kDa CO from sweet potatoes was solved and refined to 2.5 Å in the dicupric Cu(II)–Cu(II) state. The enzyme is ellipsoid in shape, with dimensions of approximately 55 by 45 by 45 Å (Figure 1a). The secondary structure is primarily  $\alpha$ -helical, with the core of the enzyme formed by a four-helix bundle composed of helices  $\alpha 2$ ,  $\alpha 3$ ,  $\alpha 6$  and  $\alpha 7$ . The helix bundle accommodates the catalytic dinuclear copper center and is surrounded by two  $\alpha$  helices,  $\alpha 1$  and  $\alpha 4$ , and several short  $\beta$  strands. Two disulfide bridges (C11 to C28 and C27 to C89) constrain the loop-rich N-terminal region of the protein (residues 1–50) to helix  $\alpha 2$ .

Both of the two active site coppers were clearly visible in the electron density maps and each is coordinated by three histidine residues contributed by the helix bundle. CuA is

Figure 1



coordinated by H88, located in the middle of helix  $\alpha 2$ , H109 and H118, located at the beginning and in the middle of helix  $\alpha 3$ , respectively (Figure 1b). The second catalytic copper, the CuB site, is coordinated by H240, H244 and H274. These residues are found at the center of helices  $\alpha 6$  and  $\alpha 7$ .

### The dicopper center in its different states

One of the key features of the CO active site is an unusual thioether bridge between C92 and H109, one of the ligands

of CuA. Apart from the geometrical restraints added to the CuA site, no function of the chemistry performed by the enzyme has been ascribed to this covalent bridge.

In the oxidized CO structure, a water molecule bridging the two copper atoms was observed, in addition to the six histidine ligands, thus forming a four-coordinate trigonal pyramidal coordination sphere for both cupric metal ions, with H109 and H240 in apical positions. This water molecule

**Figure 1**

Ribbon drawings of ibCO and its active site region. Active site ligand residues, as well as the access-controlling phenylalanine (F261), are displayed in stick representation. The atoms are colored by atom type (carbon is gray, nitrogen is blue, sulfur is yellow, oxygen is red and copper is cyan). **(a)** The front view of the 39 kDa CO. The two stabilizing disulfide bridges in the N-terminal region are displayed in yellow, whereas orange represents strands and helices are in blue. The dicopper site is found in the center of the four-helix bundle motif. Sidechains of ligands to the catalytic Cu(II)–OH–Cu(II) unit are presented as observed in the resting oxidized enzyme form. **(b)** The active site region of ibCO. Both copper sites, CuA on the left and CuB on the right, show a trigonal pyramidal coordination sphere formed by three histidine ligands and the bridging solvent molecule. The sulfur atom of C92 does not ligate the copper center, but is covalently bound to the C $\epsilon$  atom of histidine residue H109. **(c)** View of the active site region with PTU bound to the dicopper center. The sulfur of the inhibitor binds to both copper ions. In addition, the

hydrophobic cavity formed by residues I241, H244 and F261 provides van der Waals contacts with the aromatic ring of the drug. A stick representation of the active site residues of the oxidized Cu(II)–Cu(II) state of the enzyme is superimposed in blue to reveal the conformational change induced by the binding of PTU. **(d)** Superposition of the dinuclear copper center of ibCO in blue [16\*\*] with the oxygen-binding site of odgHc [23\*\*]. The metal-ligating histidine residues and copper atoms of odgHc are shown in green. The metal-ligating residues forming the CuB-binding site are completely conserved (see also, Figure 3). For the CuA-binding site, both proteins show the rare cysteine–histidine thioether bridge, with almost the same orientation of the residues. Although C2560 and H2562 are separated only by one residue in odgHc, a 17-residue-containing loop– $\beta$ -sheet region is found between C92 and H109 of ibCO (see also, Figure 3). All images have been computed using the programs SwissPdbViewer [31] and POV-Ray [http://www.povray.org/].

occupies a position 1.9 Å from CuA and 1.8 Å from CuB. We could not exclude the possibility that the water may be a chloride ion from the crystallization buffer.

The crystal structure of the reduced enzyme (2.7 Å resolution) revealed that, although the metal–metal separation increased to 4.4 Å, no other significant conformational changes were observed upon reduction of the protein. The coordination in the reduced state for CuB is square planar, with one missing coordination site. For CuA, a coordinating water molecule was found (CuA–O distance of 2.2 Å), completing the coordination sphere of CuA (trigonal planar coordinated by the three protein ligands) as a distorted trigonal pyramid.

The structure of CO with bound substrate analog inhibitor phenylthiourea (PTU) (2.7 Å resolution) was obtained by soaking crystals of the oxidized state (Figure 1c). The inhibitor complex revealed several conformational changes in the active site that indicated that access to the catalytic metal center is primarily controlled by a rotation of the aromatic ring of F261. The sulfur of PTU replaces the hydroxo bridge, present in the *met* form, and is coordinated to both copper ions, thereby increasing the metal–metal separation to 4.2 Å, compared with 2.9 Å for the oxidized form. A weak interaction between the amide nitrogen of PTU and CuB (Cu–N distance of 2.6 Å) completes the square pyramidal coordination sphere. van der Waals interactions between I241 and H244 also contribute to the high affinity of PTU for the enzyme.

### Discussion of the structure

The presence of the  $\mu$ -hydroxo group bridging the copper atoms is supported by EPR data revealing an antiferromagnetically coupled, EPR silent Cu(II)–Cu(II) state [14\*]. The observed 2.9 Å distance between the two cupric ions is very similar to that obtained using EXAFS, 2.89 Å, for the oxidized COs from *L. europaeus* and sweet potatoes, supporting an average of four N/O ligands in solution [5,14\*]. This distance seems short compared with the

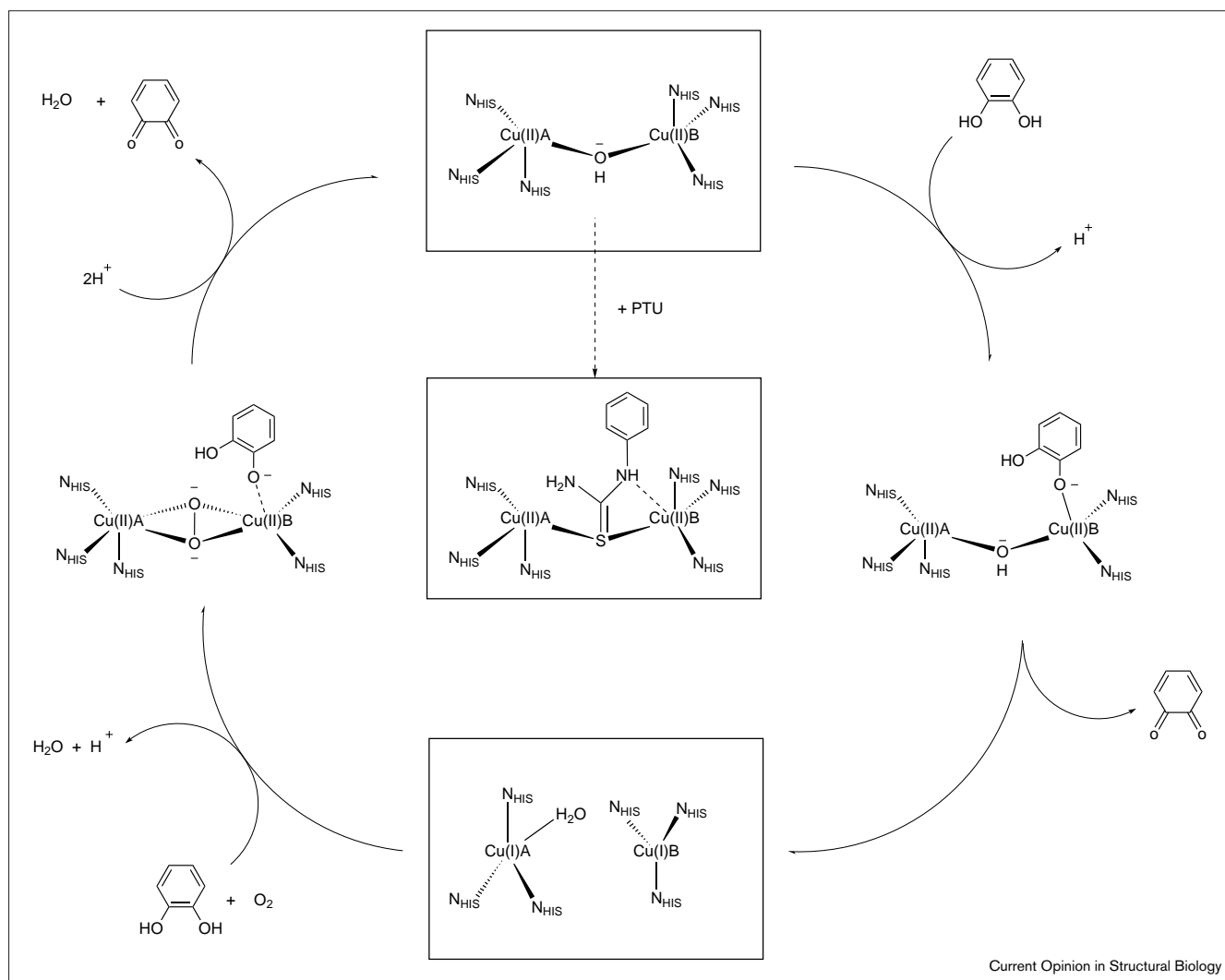
Cu(II)–Cu(II) distance in the multicopper enzyme ascorbate oxidase (3.68 Å), in which the copper ions are also singly bridged and surrounded by six histidines [17,18].

The absence of a cysteinyl–histidyl thioether bridge in human tyrosinase does not rule out its direct involvement in the electron transfer process of CO. A thioether linkage has been implicated in the catalytic activity of the mononuclear copper enzyme galactose oxidase. In this structure, the covalent bond, formed between the C $\epsilon$  carbon of a tyrosinate ligand and the sulfur of a cysteine, is proposed to stabilize the tyrosine radical generated during catalysis [19]. Although there was biochemical evidence for a cysteine–histidine thioether bridge in functional units of molluscan Hcs [20,21\*\*] and tyrosinase from *Neurospora crassa* [22] from previous reports, the crystal structure determination of *Octopus* Hc [23\*\*] provided the first three-dimensional description of this unusual bridge. The restrained geometry confirmed by this structure might allow the fast binding of the dioxygen substrate or it may optimize the electronic structure of the metal needed for its catalytic function.

### Proposed catalytic mechanism

A combination of biochemical, spectroscopic and structural data was used to propose a reaction pathway for the oxidation of two catechol molecules, coupled with the reduction of molecular oxygen to water, catalyzed by CO (Figure 2) [16\*\*]. The catalytic cycle begins with the oxidized *met* form, which is present following isolation of the enzyme. Based on the CO–PTU complex, the monodentate binding of the diphenolic substrate to CuB seems to be most likely to reduce the Cu(II)–Cu(II) form to the dicuprous state, whose structure was characterized [16\*\*]. This step is supported by the observation that stoichiometric amounts of the quinone product form immediately after the addition of catechol, even in absence of dioxygen (B Krebs, unpublished data). Because the *oxy* state of ibCO could be obtained only after the addition of H<sub>2</sub>O<sub>2</sub> and was less stable than that formed by tyrosinase [14\*], this form was excluded as the start situation.

Figure 2



Catalytic cycle of ibCO, as proposed on the basis of structural, spectroscopic and biochemical data [14•,16••]. Two molecules of catechol (or derivatives thereof) are oxidized, coupled with the reduction of molecular oxygen to water. The ternary CO–O<sub>2</sub><sup>2-</sup>–catechol complex

was modeled, guided by the binding mode observed for the inhibitor PTU. The binding mode of PTU is displayed in Figure 1c. All structurally characterized [16••] steps are boxed.

The observed binding mode for PTU and the modeled catechol-binding mode suggest that the binding of substrate and dioxygen is possible during the next step in the reaction. UV/Vis spectroscopy [14•] and preliminary resonance Raman spectra (F Tuzcek, personal communication) on *oxy* ibCO confirmed the bridging, side-on  $\mu$ - $\eta^2$ : $\eta^2$  binding mode of molecular oxygen (as peroxide) used in this model and also observed for Hcs [24].

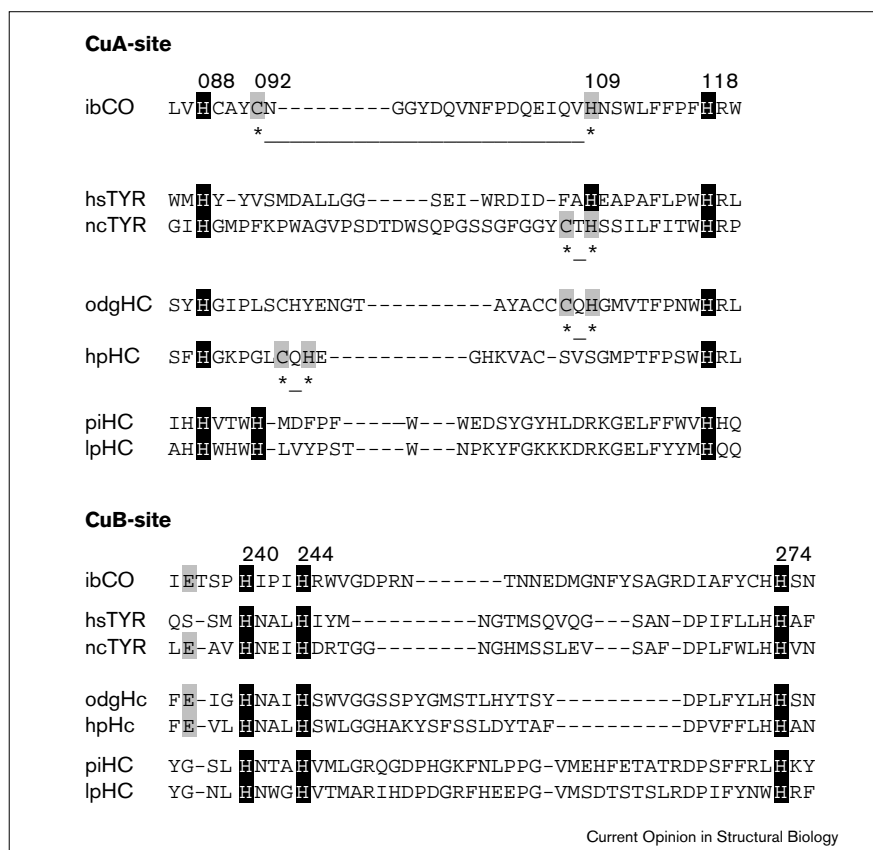
Superimposition of the aromatic ring of the modeled catechol substrate and the phenyl ring of PTU places the coordinated catechol hydroxylate group close to the ligating amide nitrogen of the inhibitor and maintains the favorable van der Waals interactions observed in the inhibitor complex. In this model, CuB would be six-coordinated with

a tetragonal planar coordination by H240, H244 and the dioxygen molecule. H274 and the catechol substrate would occupy the two axial positions in this distorted octahedral coordination, as favored by Cu(II) with nine d electrons. The CuA site would retain tetragonal pyramidal coordination, with dioxygen, H88 and H118 in equatorial positions, H109 in an axial position and a vacant nonsolvent accessible sixth coordination site. In this proposed ternary CO–O<sub>2</sub><sup>2-</sup>–substrate complex, two electrons could be transferred from the substrate to the peroxide, followed by cleavage of the O–O bond, loss of water and departure of the *o*-quinone product.

Binding of the catechol substrate to the reduced enzyme without the binding of oxygen seems less likely, as the incubation of reduced crystals did not show any catechol

**Figure 3**

Sequence alignment of the active site regions of ibCO, human tyrosinase (hsTyr), *N. crassa* tyrosinase (ncTyr), *Helix pomatia* Hc (hpHc), odgHc (subunit g), piHc and lpHc. Histidine residues ligating the dicopper center are highlighted in black. Cysteine–histidine thioether bridges, reported for the sequences of ncTyr [22], odgHc [21\*\*] and hpHc [20], are conserved in all known COs, as well as in molluscan Hcs. These bridging residues are highlighted in gray and marked by asterisks below the corresponding sequence. Residue numbers are shown for the CO from sweet potato. Whereas the coordination of the CuB site is completely conserved, residue E236 may assist in deprotonating the substrate, but is not conserved in arthropodan Hcs. In contrast, the CuA site differs among the proteins. Although H88 and H118 are strictly conserved, the third histidine ligand varies; no cysteine–histidine linkages are reported for arthropodan Hc and no trend for tyrosinases can be observed.



affinity, potentially indicating the low binding affinity of the substrate for the Cu(I)–Cu(I) center. After oxidation of the second substrate molecule and loss of the bound water, the dicopper center is in its *met* form again and ready to undergo another catalytic cycle.

### Comparison with the catalytic activity of other copper type-3 proteins

A large body of literature is available on the mechanism of tyrosinase ([3] and references therein); however, as there are no three-dimensional structures available for any tyrosinase, the basis for the differences between tyrosinase and CO remains unclear. Interestingly, more recent reports on structural work and on the catalytic activity of Hc provided the opportunity to compare Hc and CO, and to identify the residues responsible for catecholase activity.

As with CO, the locations of the dicopper center and the ligating histidines in the Hc structures from *Panulirus interruptus* (piHc) [4,25], *Limulus polyphemus* (lpHc) [26] and *Octopus dofleini* (odgHc) [21\*\*,23\*\*] are nearly identical. The C $\alpha$  positions of 64 residues of the four-helix bundle of piHc can be superimposed to the ibCO structure with an rmsd of 1.8 Å. A similar rmsd value is obtained when corresponding residues of molluscan and arthropodan Hc are superimposed [23\*\*]. For odgHc, an extended tertiary

structure similarity compared with ibCO (Figure 1d), including 704 backbone atoms, is observed (1.27 Å rmsd). In contrast to the structurally conserved CuB site (Figure 3), the varying positions of the two histidine ligands contributed by helix  $\alpha$ 3 and the optional thioether bridge result in an asymmetric disposition of the copper ligands in the copper type-3 proteins.

In arthropodan Hcs, the aromatic ring of a phenylalanine (F49 for lpHc and F75 for piHc) from the N-terminal domain shields access to the dimetal center. This phenyl ring aligns perfectly with the aromatic ring of PTU in the CO–PTU inhibitor complex [16\*\*]. Together with an additional domain present in all Hcs, the shielding of the dimetal center by the phenylalanine limits access of substrates to the dicopper center and, therefore, allows Hcs to function as oxygen transport proteins. Indeed, arthropodan Hcs show no, or only very low, catalytic activity in their native form [27]. Significant levels of monooxygenase and catecholase activity have been reported for the tarantula Hc after removing the shielding phenylalanine residue by limited proteolysis [28\*]. Higher activity has been observed for the native molluscan Hc [29\*]. In this case, the phenylalanine residue is substituted by a less bulky isoleucine, I2830 [21\*\*]. In addition, a second residue, equivalent to F261 (the so-called

'gate residue' of ibCO), is substituted by the smaller sidechain of L2689.

## Conclusions

The structural data on ibCO revealed both a close relationship between the active sites of ibCO and Hcs, and even extended homology to the molluscan Hcs. Although the CuB site is strictly conserved for all copper type-3 proteins, the varying CuA environment seems to tune the proteins to specific activities. Based on the structural data for the substrate analog inhibitor, we favor the monodentate binding of the substrate molecule to the CuB site, rather than a bidentate mode, as postulated for the catecholase activity of tyrosinase [3]. As tyrosinase shows a higher binding affinity for dioxygen and is also present in the *oxy* form (10–15%) after isolation [3], it remains to be evaluated whether the proposed mechanism for CO can also be applied to the catecholase activity of tyrosinase.

As no structural data from any tyrosinase are available so far, comparative <sup>1</sup>H NMR studies on ibCO with respect to recent data obtained from *Streptomyces antibioticus* tyrosinase [30•] are under way (GW Canters, personal communication) and hold the promise to finally reveal differences in their active sites.

## Acknowledgements

Supported by the Welch Foundation, the National Institutes of Health, the Deutsche Forschungsgemeinschaft and the Fonds der Chemischen Industrie. Thanks are due to Marianne E Cuff for sharing the coordinates of odgHc and Carsten Gerdemann for helpful discussions.

## References and recommended reading

Papers of particular interest, published within the annual period of review, have been highlighted as:

- of special interest
- of outstanding interest

1. Karlin KD: **Metalloenzymes, structural motifs, and inorganic models.** *Science* 1993, **261**:701-708.
  2. Solomon EI, Tuzcek F, Root DE, Brown CA: **Spectroscopy of binuclear dioxygen complexes.** *Chem Rev* 1994, **94**:827-856.
  3. Solomon EI, Sundaram UM, Machonkin TE: **Multicopper oxidases and oxygenases.** *Chem Rev* 1996, **96**:2563-2605.
  4. Gaykema WPJ, Hol WGJ, Vereijken JM, Soeter NM, Bak HJ, Beintema JJ: **3.2 Å structure of the copper-containing, oxygen-carrying protein *Panulirus interruptus* haemocyanin.** *Nature* 1984, **309**:23-29.
  5. Rompel A, Fischer H, Büldt-Karentzopoulos K, Meiwes D, Zippel F, Nolting HF, Hermes C, Krebs B, Witzel H: **Spectroscopic and EXAFS studies on catechol oxidases with dinuclear copper centers of type 3: evidence for  $\mu$ - $\eta^2$ :  $\eta^2$ -peroxo-intermediates during the reaction with catechol.** *J Inorg Biochem* 1995, **59**:715.
  6. Pierpoint WS: ***o*-Quinones formed in plant extracts.** *Biochem J* 1969, **112**:609-616.
  7. Dervall BJ: **Phenolase and pectic enzyme activity in the chocolate spot disease of beans.** *Nature* 1961, **189**:311.
  8. Walker JRL, Ferrar PH: **Diphenol oxidases, enzyme-catalysed •• browning and plant disease resistance.** *Biotechnol Genet Eng Rev* 1998, **15**:457-497.
- The most recent and detailed review about the proposed functions of catechol oxidases.
9. Trémolières M, Bieth JG: **Isolation and characterization of the polyphenoloxidase from senescent leaves of black poplar.** *Phytochemistry* 1984, **23**:501-505.
  10. Krebs B: **Purple acid phosphatases and catechol oxidase and their model compounds. Crystal structure of purple acid phosphatase from kidney beans.** In *Bioinorganic Chemistry: An Inorganic Perspective of Life*. Edited by Kessissoglou DP. Dordrecht, Kluwer Academic Publishers: 1995:371-384.
  11. Mayer AM, Harel E: **Polyphenol oxidases in plants.** *Phytochemistry* 1979, **18**:193-215.
  12. van Gelder CWG, Flurkey WH, Wichers HJ: **Sequence and structural features of plant and fungal tyrosinases.** *Phytochemistry* 1997, **45**:1309-1323.
  13. Rompel A, Fischer H, Meiwes D, Büldt-Karentzopoulos K, Magrini A, Eicken C, Gerdemann C, Krebs B: **Substrate specificity of catechol oxidase from *Lycopus europaeus* and characterization of the bioproducts of enzymic caffeic acid oxidation.** *FEBS Lett* 1999, **445**:103-110.
  14. Eicken C, Zippel F, Büldt-Karentzopoulos K, Krebs B: **Biochemical • and spectroscopic characterization of catechol oxidase from sweet potatoes (*Ipomoea batatas*) containing a type-3 dicopper center.** *FEBS Lett* 1998, **436**:293-299.
- This paper reports the first isolation and characterization, including UV/Vis and extended X-ray absorption fine structure (EXAFS), of catechol oxidase (CO) from sweet potatoes. The current mechanism for CO is based on these and the structural data [16••].
15. Rompel A, Fischer H, Meiwes D, Büldt-Karentzopoulos K, Dillinger R, Tuzcek F, Witzel H, Krebs B: **Purification and spectroscopic studies on catechol oxidases from *Lycopus europaeus* and *Populus nigra*: evidence for a dinuclear copper center of type 3 and spectroscopic similarities to tyrosinase and hemocyanin.** *J Biol Inorg Chem* 1999, **4**:56-63.
  16. Klabunde T, Eicken C, Sacchettini JC, Krebs B: **Crystal structure of a •• plant catechol oxidase containing a dicopper center.** *Nat Struct Biol* 1998, **5**:1084-1090.
- The structure of catechol oxidase from sweet potatoes in different states is reported and a mechanism for the catalytic cycle is proposed. This is the first structural report of a copper type-3 enzyme.
17. Messerschmidt A, Rossi A, Ladenstein R, Huber R, Bolognesi M, Gatti G, Marchesini A, Petruzelli R, Finazzi-Agro A: **X-ray crystal structure of the blue oxidase ascorbate oxidase from zucchini. Analysis of the polypeptide fold and a model of the copper sites and ligands.** *J Mol Biol* 1989, **206**:513-529.
  18. Messerschmidt A, Ladenstein R, Huber R, Bolognesi M, Avigliano L, Petruzelli R, Rossi A, Finazzi-Agro A: **Refined crystal structure of ascorbate oxidase at 1.9 Å resolution.** *J Mol Biol* 1992, **224**:179-205.
  19. Ito N, Phillips SEV, Stevens C, Ogel ZB, McPherson MJ, Keen JN, Yadav KDS, Knowles PF: **Novel thioether bond revealed by a 1.7 Å crystal structure of galactose oxidase.** *Nature* 1991, **350**:87-90.
  20. Gielens C, De Geest N, Xin XQ, Devreese B, Van Beeumen J, Preaux G: **Evidence for a cysteine-histidine thioether bridge in functional units of molluscan haemocyanins and location of the disulfide bridges in functional units d and g of the betaC-haemocyanin of *Helix pomatia*.** *Eur J Biochem* 1997, **248**:879-888.
  21. Miller KI, Cuff ME, Lang WF, Varga-Weisz P, Field KG, van Holde KE: **•• Sequence of the *Octopus dofleini* hemocyanin subunit: structural and evolutionary implications.** *J Mol Biol* 1998, **278**:827-842.
- This publication includes the first structure of a molluscan hemocyanin and a detailed discussion of the data.
22. Lerch K: **Primary structure of tyrosinase from *Neurospora crassa*. II. Complete amino acid sequence and chemical structure of a tripeptide containing an unusual thioether.** *J Biol Chem* 1982, **257**:6414-6419.
  23. Cuff ME, Miller KI, van Holde KE, Hendrickson WA: **Crystal structure •• of a functional unit from *Octopus* hemocyanin.** *J Mol Biol* 1998, **278**:855-870.
- This paper describes the first complete sequence of a molluscan hemocyanin.
24. Magnus KA, Hazes B, Ton-That H, Bonaventura C, Bonaventura J, Hol WGJ: **Crystallographic analysis of oxygenated and desoxygenated states of arthropod hemocyanin shows unusual differences.** *Proteins* 1994, **19**:302-309.
  25. Volbeda A, Hol WGJ: **Crystal structure of hexameric haemocyanin from *Panulirus interruptus* refined at 3.2 Å resolution.** *J Mol Biol* 1989, **209**:249-279.
  26. Hazes B, Magnus KA, Bonaventura C, Bonaventura J, Dauter Z, Kalk KH, Hol WGJ: **Crystal structure of desoxygenated *Limulus polyphemus***

subunit II hemocyanin at 2.18 Å resolution: clues for the mechanism for allosteric regulation. *Protein Sci* 1993, 2:597-619.

27. Zlateva T, Di Muro P, Salvato B, Beltramini M: **The o-diphenol activity of arthropod hemocyanin.** *FEBS Lett* 1996, **384**:251-254.

28. Decker H, Rimke T: **Tarantula hemocyanin shows phenoloxidase activity.** *J Biol Chem* 1998, **273**:25889-258892.

The influence of the shielding by a phenylalanine residue in the active sites of arthropodan hemocyanins is reported in this publication. This residue blocks the substrate access to the dicopper center and therefore permits the functioning of arthropodan hemocyanins as oxygen transport proteins.

29. Salvato B, Santamaria M, Beltramini M, Alzuet G, Casella L: **The enzymatic properties of *Octopus vulgaris* hemocyanin: o-diphenol oxidase activity.** *Biochemistry* 1998, **6**:14065-14077.

Catecholase activity for a native molluscan hemocyanin is shown and a detailed mechanism is proposed.

30. Bubacco L, Salgado J, Tepper AWJW, Vijgenboom E, Canters GW: **<sup>1</sup>H NMR spectroscopy of the binuclear site of *Streptomyces antibioticus* tyrosinase.** *FEBS Lett* 1999, **442**:215-220.

This publication is the first report of a paramagnetic NMR study of a type-3 copper protein and gives the final proof that the copper atoms in tyrosinase are surrounded by six histidine ligands.

31. Guex N, Peitsch MC: **SWISS-MODEL and the Swiss-Pdb Viewer: an environment for comparative protein modeling.** *Electrophoresis* 1997, **18**:2714-2723.